Supplementary information

Establishing the gain-of-Notch model in *Apc^{min}*-background mice to examine the role of Notch signaling in intestinal tumorigenesis.

We generated an intestinal gain-of-Notch model in *Apc^{min}* mice by crossing these mice with *Rosa-N1icd* (*RN1*) mice, which contain a transgene composed of a floxed Neo/STOP cassette followed by N1icd without the PEST domain in the *Rosa26* locus (1) carrying a *Vil-Cre* transgene (2). These mice have Notch-activated intestinal epithelium in which intestinal tumors will occur upon the loss of heterogeneity of the *Apc^{min}* locus.

It is well known that no tumors have been observed in the intestines of *Vil-Cre;RosaN1$^{+/RN1}$* mice (3). Tumors are observed only when *Vil-Cre;RosaN1$^{+/RN1}$* mice are crossed with *Apc^{min}* mice. Therefore, we were assured that tumor formation in *Vil-Cre;RosaN1$^{+/RN1}$;Apc^{min}* mice was caused by the loss of heterozygosity (LOH) in the Apc locus. To confirm the status of the second Apc allele in *Vil-Cre;RosaN1$^{+/RN1}$;Apc^{min}*, we isolated the tumors from both *Vil-Cre;RosaN1$^{+/RN1}$;Apc^{min}* and control *Apc^{min}* mice using laser microdissection and investigated whether LOH occurred in the tumors. Genomic PCR analysis revealed that the second wild-type APC allele was inactivated in the polyps of *Vil-Cre;RosaN1$^{+/RN1}$;Apc^{min}* mice (Supplementary Figure 1A). Moreover, we also observed that expression of the APC protein was absent in Notch-activated *Apc^{min}* tumors using an antibody that detects the C-terminal region of the APC protein (Supplementary Figure 1B). These results showed that tumor formation in *Vil-Cre;RosaN1$^{+/RN1}$;Apc^{min}* is caused by LOH of the APC locus, not by Notch activity.

It was previously reported that *Vil-Cre;RosaN1$^{+/RN1}$;Apc^{min}* mice show postnatal lethality within 3 days of birth (4). In this study, however, we used a different *Vil-Cre* transgenic line to activate Notch signaling (2). *Vil-Cre;RosaN1$^{+/RN1}$;Apc^{min}* mice generated in this study could survive longer than 12 weeks. The discrepancy in lethality between these independent models may have been due to differences in *Vil-Cre* transgenic mice. While the *Vil-Cre* mice used by the Fre et al. have Cre activity in the kidney as well as in the intestine (5), *Vil-Cre* mice used in this study had Cre activity in the intestine, but not the kidney (2). In our previous paper (3), we reported the deletion efficiency of our *Vil-Cre* transgenic mice.

The effects of DAPT on the expression of Wnt target genes in *NRARP$^{low/-}$* CRCLs

We treated the *NRARP$^{low/-}$* CRCLs, SW620 and COLO205, with DAPT and first examined

the expression levels of *CDX1, CDX2* and *VIMENTIN.* As expected, we could not detect any significant difference in both cell lines after DAPT treatment (Supplementary Figure 6A). We next performed the chromatin-immunoprecipitation experiment to detect the epigenetic status of *NRARP*$^{low/-}$ cell lines, SW620 after DAPT treatment. We also did not detect significant difference in the binding affinity of β-catenin/TCF4 to the promoters and also the status of histone methylation at the H3K27me3, H3K9me3 and H3K4me3 (Supplementary Figure 6B). We further examined the expression levels of Wnt/β-catenin target genes, *PROX1*, *AXIN2*, *c-MYC*, and *APCDD1*, by DAPT treatment. As expected, we could not detect any significant difference between groups (Supplementary Figure 6C). These results are well correlated with the expression levels of N1ICD and NRARP (Figure 5B). Thus, we concluded that the DAPT treatment in the *NRARP*$^{low/-}$ cell lines did not further affect the epigenetic status and characteristics of these cells.

Supplemental experimental procedures

APC allelic loss analysis

Microdissected normal and tumor tissues in *Apc*^{min} and *Vil-Cre;RosaN1*$^{+/RN1}$*;Apc*^{min} mice were digested in 50 μL lysis buffer containing 500 μg/mL proteinase K. LOH of the Apc gene was examined using genomic PCR. Primer sequences were as follows: *Apc* wild type 5′-GCCATCCCTTCACGTTAG-3′; *Apc*^{min} 5′-TTCTGAGAAAGACAGAAGTTA-3′; *Apc* Common 5′-TTCCACTTTGGCATAAGGC-3′. PCR products from the tissues with LOH displayed only one band from the *Apc*^{min} allele.

Chromatin immunoprecipitation (ChIP) and primer pairs for ChIP

ChIP analyses were performed using the EZ-Chip kit according to the manufacturer's protocol (Upstate Biotechnology, Millipore, Billerica, MA). Immune complexes were isolated and 1 μL of immunoprecipitated purified DNA was used real-time PCR. Primer sequences were as follows: *PROX1* primers (6) fwd 5′-CCAATCGCATTCATGTGACA-3′; rev 5′-TTCCTGCCTGAAGAAGTCC-3′. *AXIN2* primers (6) fwd 5′-AGTGTGCAGGGAGCTCAGAT-3′; rev 5′-AGGTGGGGAGAGAGAAAAGG-3′. *c-MYC* primers (7) fwd 5′-TCTCCCTGGGACTCTTGATCA-3′; rev 5′-TTTGACAAACCGCATCCTTGT-3′. *APCDD1*

primers (8) fwd 5′-GGGAAACTCTTCCTGCCTTT-3′; rev 5′-AGAAACGCTCCCTGTCAGTC-3′.

Primer pairs for RT-PCR analysis

Primer sequences were as follows: *Axin2* primers fwd 5′-GCTGGAGAAACTGAAACTGGA-3′; rev 5′-CAAAGTGTTGGGTGGGGTAAG-3′. *Wif1* primers fwd 5′-GCCACGAACCCAACAAGT-3′; rev 5′-TCCCTTCTATCCTCAGCCTTT-3′. *Nkd1* primers fwd 5′-ACTCAGGATGGGAGCAAGC-3′; rev 5′-AGACAGTATGGGTGGTGGTA-3′. *Apcdd1* primers fwd 5′-ATGAACACCACCCTCCCATAC-3′; rev 5′-GTAGTAATGCCCTTCCCAGGT-3′. *TNR (GFP)* primers fwd 5′-ATGGTGAGCAAGGGCGAGGA-3′; rev 5′-TTACTTGTACAGCTCGTCCA-3′. *Nrarp* primers fwd 5′-GCGTGGTTATGGGAGAAAGAT-3′; rev 5′-GGGAGAGGAAAAGAGGAATGA-3′. *Hes1* primers fwd 5′-GTGGGTCCTAACGCAGTGTC-3′; rev 5′-TCAGAAGAGAGAGGTGGGCTA-3′. *NRARP* primers fwd 5′-GGGCTGCATAGAAAATTGGA-3′; rev 5′-CCCTTTTTAGCCTCCCAGAG-3′. *CDX1* primers fwd 5′-AGACTCTGCCCCCTTCTCTC-3′; rev 5′-CCTGCAGCCTCACTTCTACC-3′. *CDX2* primers fwd 5′-AGACCAACAACCCAAACAGC -3′; rev 5′-CCCGAACAGGGACTTGTTTA-3′. *VIMENTIN* primers fwd 5′-TCCAGCAGCTTCCTGTAGGT-3′; rev 5′-GAGAACTTTGCCGTTGAAGC-3′. *PROX1* primers fwd 5′-TGGGCTCTGAAATGGATAGG -3′; rev 5′-CCACTGACCAGACAGAAGCA-3′. *AXIN2* primers fwd 5′-CAAACTCATCGCTTGCTTTTT-3′; rev 5′-CACTTACTTTTTCTGTGGGGAAG-3′. *c-MYC* primers fwd 5′-CGTAGTTGTGCTGATGTGTGG-3′; rev 5′-CTCGGATTCTCTGCTCTCCTC-3′. *APCDD1* primers fwd 5′-ATCACAGTCCCAAACCAACTC-3′; rev 5′-ACTTTTCCTGCCATTTTCCTG-3′. *MMP2* primers fwd 5′-TATGACAGCTGCACCACTGAG-3′; rev 5′-TATTTGTTGCCCAGGAAAGTG-3′. *NLK* primers fwd 5′-GCTGGATATTGAGCCGGATA-3′; rev 5′-CATCTTCAATTCCCGGAAGA-3′. *SETDB1* primers fwd 5′-CGAATTCTGGGCAAGAAGAG-3′; rev 5′-TCAGCAGGAGGGTGGTAATC-3′.

Supplemental Figure Legends

Supplemental Figure 1. Loss of heterogeneity of the *Apc^{min}* locus in Notch-activated *Apc^{min}* tumors.

(A) Apc LOH analysis of tumors in *Apc*^{min} (APC) and *Vil-Cre;RosaN1*$^{+/RN1}$*;Apc*^{min} (APC;N1). The upper band represents the wild-type *Apc* allele, whereas the lower band represents an *Apc* ^{min} PCR product. N, normal tissue; T, tumor.

(B) Hematoxylin and APC immunostaining of APC and APC;N1 tumors. Note that the expression levels of APC was absent in both APC and APC;N1 tumors. N, normal tissue; T, tumor. Dotted lines indicate tumor regions. Scale bars, 50 μm.

Supplemental Figure 2. The effects of Notch signaling on the growth of CRCLs.

(A, B) The growth of DAPT treated *NRARP*^{high} CRCLs or ΔEN1-overexpressing *NRARP*$^{low/-}$ CRCLs. *NRARP*^{high} SNU61 and LOVO cells were treated daily with vehicle or 1μM DAPT. *NRARP*$^{low/-}$ COLO205 and SW620 cells were transfected with 2 μg of mock or ΔEN1. Cell proliferation was assessed using a Cell Counting Kit-8 (Dojindo Laboratories). Note that Notch signaling activity suppresses the growth of the CRCLs.

Supplemental Figure 3. Chromatin immunoprecipitation analysis of the *PROX1, AXIN2*, and *c-Myc* promoter regions in LOVO cells. Soluble chromatin was prepared from DAPT-treated (left panels) or DN-MAML-expressing (right panels) cells and was immunoprecipitated using the indicated antibodies. Final DNA extracts were amplified using pairs of primers that cover the TCF4/β-catenin binding site in the Wnt target gene promoters using real-time PCR. Bars, mean (SD). $P < 0.05$ (*) and $P < 0.001$ (**).

Supplemental Figure 4. Chromatin immunoprecipitation analysis of Wnt target genes (*PROX1*, *AXIN2*, *c-MYC*, and *APCDD1*) in SW620 cells. Soluble chromatin was prepared from mock-expressing or ΔEN1-expressing cells and was immunoprecipitated using the indicated antibodies. Final DNA extracts were amplified, using pairs of primers that cover the TCF4/β-catenin binding site in the Wnt target gene promoters, using real-time PCR. Bars are mean (SD). $P < 0.05$ (*) and $P < 0.001$ (**).

Supplemental Figure 5. Knockdown of *NLK1* and *SETDB1* by *NLK* siRNA and *SETDB1* siRNA. Quantitative real-time RT-PCR **(A)** and western blot **(B)** analyses of *NLK1* and *SETDB1* in *NRARP*$^{low/-}$ SW620 cells transfected with control siRNA, *NLK* siRNA and *SETDB1* siRNA for 48 h. β-Actin was used for normalization.

Supplemental Figure 6. The effects of DAPT on the expression of Wnt target genes in *NRARP*$^{low/-}$ CRCLs

(A) Quantitative real-time RT-PCR analysis of *CDX1*, *CDX2*, and *VIMENTIN* in *NRARP*$^{low/-}$ CRCLs. SW620 and COLO205 cells were treated daily with vehicle or 1μM DAPT. Levels of *CDX1*, *CDX2*, and *VIMENTIN* transcripts were measured after 48 hrs.
(B) Chromatin immunoprecipitation and PCR analysis of promoter regions of Wnt target genes in *NRARP*$^{low/-}$ SW620 cells. SW620 cells were daily treated with vehicle and 1 μM DAPT for 48 hrs. Soluble chromatin prepared from each cultured cells was immunoprecipitated with indicated antibodies. The final DNA extracts were amplified using pairs of primers that cover the Wnt/β-catenin binding sites in promoter regions of Wnt target genes.
(C) Quantitative real-time RT-PCR analysis of Wnt target genes in DAPT-treated *NRARP*$^{low/-}$ CRCLs. SW620 and COLO205 cells were treated daily with vehicle or 1 μM DAPT. Levels of PROX1, *AXIN2*, *c-MYC* and *APCDD1* transcripts were measured after 48 hrs.

Supplemental Table 1. Gene list of T-DEG and Notch-DEG. N, normal intestinal epithelium; N_Notch+, Notch-activated intestinal epithelium; T, tumor; T_Notch+, Notch-activated tumor. Each group contains 2 biological replicas.

Supplemental Table 2. Results of KEGG pathway analysis using cluster A (Figure 2A).

Supplemental Table 3. Results of KEGG pathway analysis using cluster B (Figure 2A).

Supplemental Table 4. List of genes in mouse DEG∩human NRARP CO-DEG. N, normal intestinal epithelium; N_Notch+, Notch-activated intestinal epithelium; T, tumor; T_Notch+, Notch-activated tumor. Each group contains 2 biological replicas.

Supplemental references

1. Murtaugh, L.C., Stanger, B.Z., Kwan, K.M., and Melton, D.A. 2003. Notch signaling controls multiple steps of pancreatic differentiation. *Proc Natl Acad Sci U S A* 100:14920-14925.
2. Madison, B.B., Dunbar, L., Qiao, X.T., Braunstein, K., Braunstein, E., and Gumucio, D.L. 2002. Cis elements of the villin gene control expression in restricted domains of the vertical (crypt) and horizontal (duodenum, cecum) axes of the intestine. *J Biol Chem* 277:33275-33283.

3. Koo, B.K., Lim, H.S., Chang, H.J., Yoon, M.J., Choi, Y., Kong, M.P., Kim, C.H., Kim, J.M., Park, J.G., and Kong, Y.Y. 2009. Notch signaling promotes the generation of EphrinB1-positive intestinal epithelial cells. *Gastroenterology* 137:145-155, 155 e141-143.
4. Fre, S., Huyghe, M., Mourikis, P., Robine, S., Louvard, D., and Artavanis-Tsakonas, S. 2005. Notch signals control the fate of immature progenitor cells in the intestine. *Nature* 435:964-968.
5. el Marjou, F., Janssen, K.P., Chang, B.H., Li, M., Hindie, V., Chan, L., Louvard, D., Chambon, P., Metzger, D., and Robine, S. 2004. Tissue-specific and inducible Cre-mediated recombination in the gut epithelium. *Genesis* 39:186-193.
6. Petrova, T.V., Nykanen, A., Norrmen, C., Ivanov, K.I., Andersson, L.C., Haglund, C., Puolakkainen, P., Wempe, F., von Melchner, H., Gradwohl, G., et al. 2008. Transcription factor PROX1 induces colon cancer progression by promoting the transition from benign to highly dysplastic phenotype. *Cancer Cell* 13:407-419.
7. Beiter, K., Hiendlmeyer, E., Brabletz, T., Hlubek, F., Haynl, A., Knoll, C., Kirchner, T., and Jung, A. 2005. beta-Catenin regulates the expression of tenascin-C in human colorectal tumors. *Oncogene* 24:8200-8204.
8. Takahashi, M., Fujita, M., Furukawa, Y., Hamamoto, R., Shimokawa, T., Miwa, N., Ogawa, M., and Nakamura, Y. 2002. Isolation of a novel human gene, APCDD1, as a direct target of the beta-Catenin/T-cell factor 4 complex with probable involvement in colorectal carcinogenesis. *Cancer Res* 62:5651-5656.

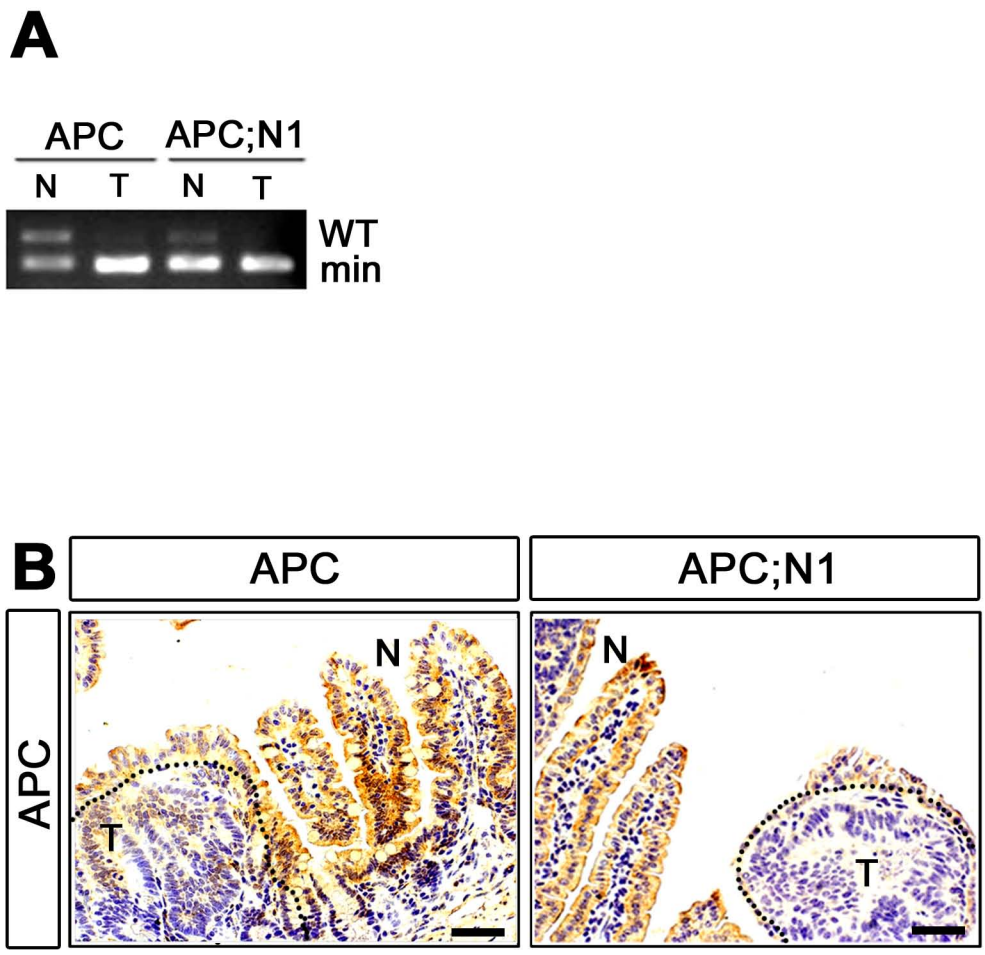

Supplementary Figure 1 Kim *et al*

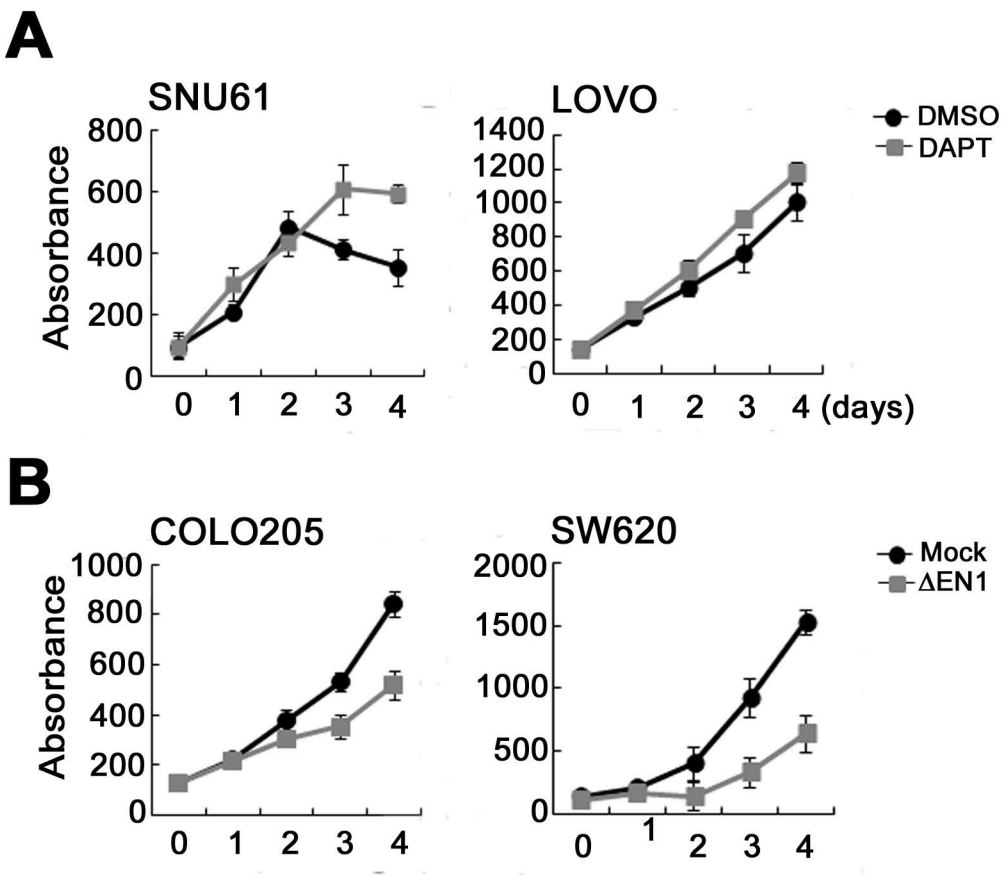

Supplementary Figure 2 Kim *et al*

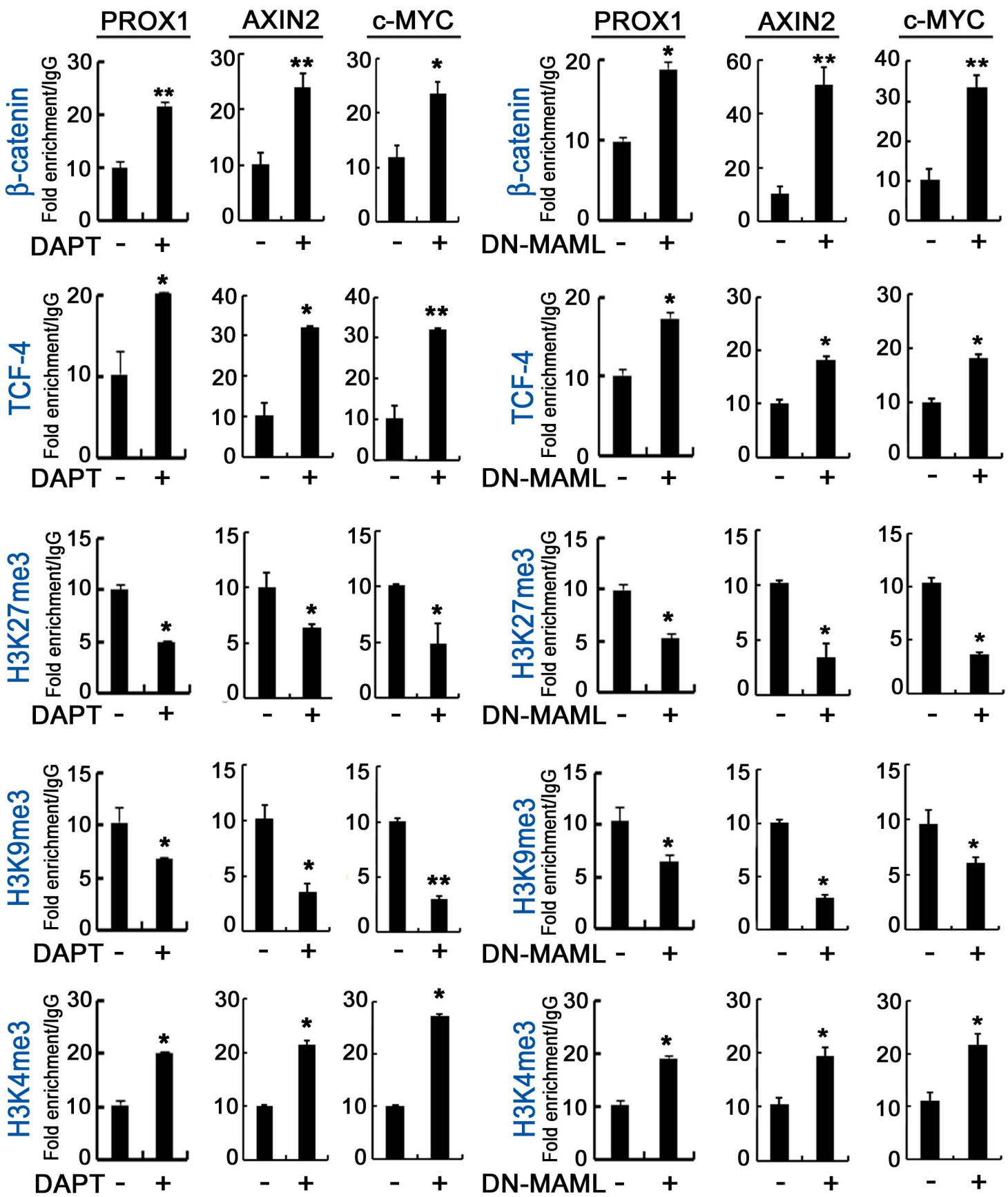

Supplementary Figure 3 Kim *et al*

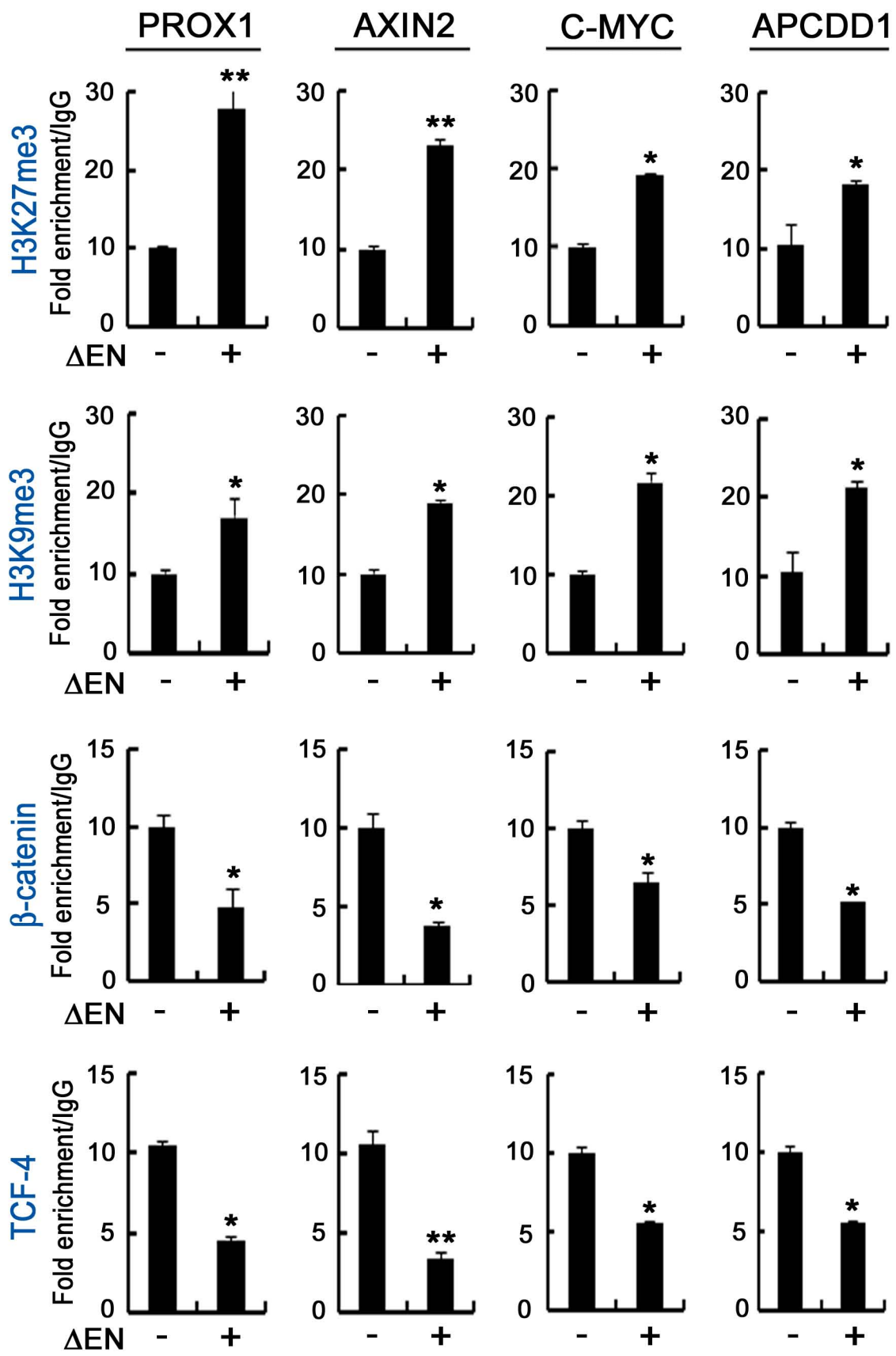

Supplementary Figure 4 Kim *et al.*

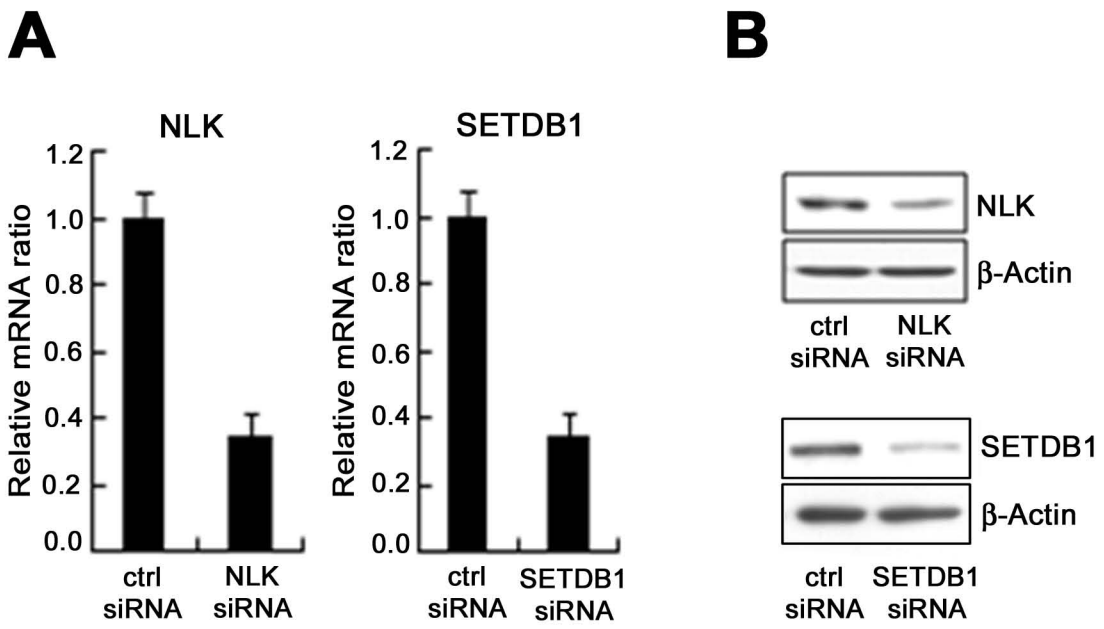

Supplementary Figure 5 Kim *et al.*

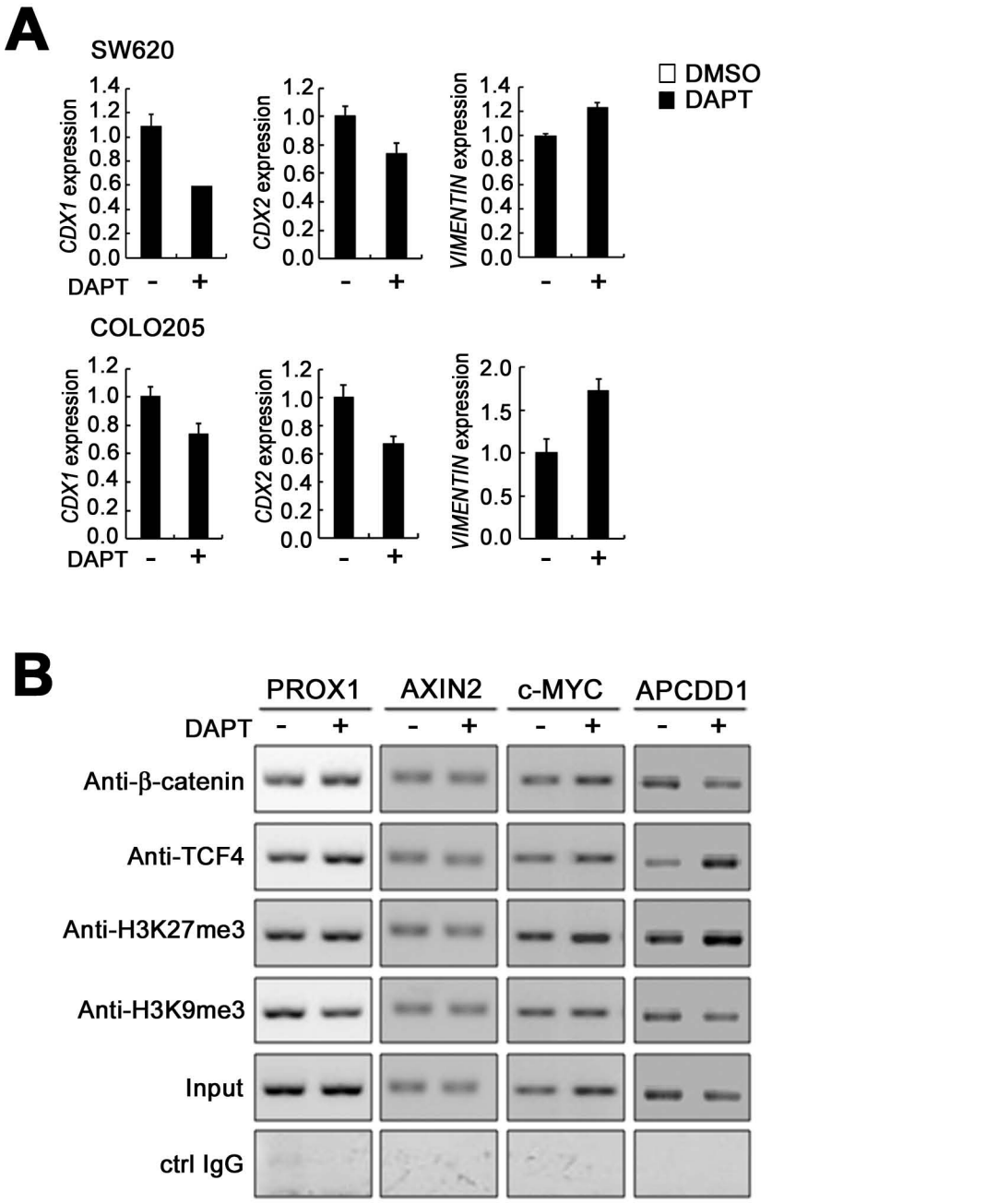

Supplementary Figure 6 Kim *et al*